LEADING-EDGE 'VORTEX FLAPS' FOR ENHANCED SUBSONIC AERODYNAMICS OF SLENDER WINGS*

ICAS-80-13.5

Dhanvada M. Rao
President, Vigyan Research Associates, Inc.
Hampton, Va., USA

Abstract

The 'Vortex Flap' is a novel concept aimed at reducing the lift-dependent drag due to leading-edge flow separation on highly swept, slender wings at high angles of attack. The suction effect of coiled vortices generated via controlled seperation over leading-edge flap surfaces is utilized to produce an aerodynamic thrust component. This principle was verified through wind-tunnel experiments on 74-deg. and 60-deg. delta wings and a supersonic-cruise slender wing aircraft configuration. Adaptation of the vortex-flap for augmentation of roll-control on the 74-deg. delta at high angles of attack also was demonstrated. Selected results are presented in this paper to indicate the potential of the vortex flap concept to enhance the low-speed performance, stability and control of slender wing aircraft.

I. Introduction

Highly-swept slender wings employed on supersonic cruise aircraft and missles are characteristically inefficient in the subsonic phases of flight such as climb to cruise, combat maneuver, loiter and approach to landing. At the relatively high angles of attack during these operations, flow separation from the leading edges generates vortices which provide additional lift but at a high cost in drag due to loss of leading-edge suction. A forward movement of the center of vortex lift with increasing angle of attack causes longitudinal instability, eventually leading to pitch-up due to breakdown of the vortices. The vortex system also markedly influences lateral and directional stability characteristics of the slender-wing aircraft and often interferes with aft control surfaces.

Leading-edge devices such as flaps, slats etc. found effective in maintaining attached flow to higher angles of attack on moderately swept wings have not been equally successful when applied to slender planforms. Cambering a highly-swept leading edge for attached flow at high angles of attack results in a complex geometry, and to achieve it in practice by deflecting the leading-edge structure from its cruise shape would undoubtedly entail considerable mechanical complexity and weight penalty. Due to large deflection angles involved, separation along the knee-line is likely so that complete vortex suppression may not be possible even with attached flow at the leading-edge.

This paper presents a new concept, the 'vortex flap', which aims to exploit rather than suppress the natural tendency towards flow separation and vortex formation at highly swept leading edges, and thus offers a more rational approach to flow management for improved subsonic efficiency of slender wings at high angles of attack. Selected results will be presented from a series of wind tunnel model tests on simple research wings as well as a realistic slender supersonic aircraft configuration to indicate the drag-reduction potential of the vortex flap and its impact on other important low-speed aerodynamic characteristics.

II. The Vortex Flap

The vortex flap physically resembles a conventional leading-edge flap but its aerodynamic functioning is quite different, fig. 1. While the conventional flap is adjusted to match the upwash in order to achieve a smooth on-flow, the vortex flap is deliberately under-deflected so as to force separation on its upper surface. The resultant coiled vortex, stabilized by the large sweep angle, is maintained on the flap all along the span and thus a significant thrust component is derived from the vortex suction. The flap angle is adjusted in conjunction with the angle of attack to bring the attachment streamline on the knee. Thus, not only is the whole flap brought under the vortex suction but simultaneously a smooth entry and attached flow ensured on the wing upper surface. The upper part of fig. 1 presents a composite sketch to contrast the flow fields of the basic wing and the vortex flap.

Two alternate embodiments of the vortex flap principle are indicated in fig. 1: a conventional inboard hinged flap (A), and an extendable or folding flap (B) which is retracted flush with the wing undersurface. On a wing having sharp supersonic leading edges the type-A flap will be preferred for simplicity, whereas on a more highly swept planform where blunt leading edges can be used to recover subsonic leading-edge suction in supersonic cruise, the type-B flap will provide the necessary sharp separation edge.

The various flow regimes associated with the vortex flap (viewed in the plane normal to leading edge) and their position on the drag polar are qualitatively indicated in fig. 2. At a constant flap deflection, increasing angle of attack will produce successive flow patterns as follows:

A. Flap over-deflected relative to the small upwash; flow separation behind the flap; high drag.

B. Flap angle matches the upwash; smooth on-flow but possible knee separation.

C. Upwash marginally exceeds flap deflection; separation and small vortex on flap upper surface but attachment still on flap; knee separation still likely.

*This research was supported by NASA Langley Research Center

D. Attachment at knee; flap fully under vortex; knee separation eliminated; optimum vortex flap operation.

E. Attachment shifts to the wing; vortex moves off the flap; thrust effectiveness declines.

The various stages of flow development in the order shown in fig. 2 may also be found with increasing outboard distance on the flap at constant deflection and angle of attack, due to increasing upwash angle towards the tip. In addition, the vortex core will normally expand due to mass entrainment and viscous effects. Ideally, a twisted and inversely tapered flap (i.e. with deflection and chord increasing towards the tip) will accommodate this spanwise development to maintain the optimum vortex flow pattern all along the flap span. A more practical approach however may be to have a number of spanwise flap segments, each deflected independently according to a schedule approximating the ideal flap twist for maximum thrust performance.

III. Discussion of Results

The wind-tunnel tests were carried out at NASA Langley Research Center in the 7-ft. x 10-ft. high speed tunnel at low subsonic Mach numbers. A review of selected experimental results from the different test models will be presented to highlight the capabilities of the basic vortex flap concept and its adaptations.

74-Deg. Planar Delta Wing

The initial proof-of-concept experiments on the vortex flap were conducted during 1978 on a flat-plate delta wing model with a blunt, constant-radius leading edges swept at 74 deg. The model details, flap configurations and test data are presented in ref. 1. The model simulated an extended vortex flap arrangement (type B, fig. 2). Starting with a constant-chord, full-length flap a series of configurations were tested, the variables including flap deflection angle, hinge-line distance from the leading edge (of interest from structural considerations), flap length (or spanwise coverage) and inverse-taper planform. Partial results of this study are summarized in terms of lift/drag ratio (as a basic performance parameter) in fig. 3 and briefly discussed below. Note that the lift coefficient is based on the total projected plan area (i.e. wing plus flap); accordingly the comparisons in fig. 3 should essentially reflect the aerodynamic effects of the flap variables investigated.

The effect of increasing flap deflection angle is seen mainly at lift coefficients less than 0.4 where adverse flow separation (see fig. 2, A) leads to a pronounced drag increase at the higher deflection angle. At C_L of 0.5 and greater, however, the vortex flap performance is essentially invariant between 30-deg. and 45-deg. deflections.

Increasing hinge-line set-back distance progressively reduces the vortex flap effectiveness. This detrimental effect probably is related to the decreasing upwash with distance away from the leading edge, which will cause the flow on the backset flap to tend towards adverse separation of fig. 2, A.

Removing the first 25-percent of the flap length from the apex (as an arbitrary first step) improved L/D at lift coefficients below 0.3 while the performance was unchanged at higher lift. The forward portions of the vortex flap evidently are dispensable due to the low upwash level and limited thrust potential in the very inboard regions of the wing.

Finally, an inverse-taper vortex flap produced essentially the same level of L/D improvement over the whole C_L-range as the constant-chord flap in spite of nearly 36-percent less flap area, thus emerging as a more efficient vortex-flap planform as expected.

The longitudinal aerodynamic characteristics of 74-deg. delta wing with and without tapered vortex flap are compared in fig. 4. The lift coefficient here is based on the basic wing area. It is instructive to compare the pairs of data at constant angles of attack (shown linked with angle of attack identified). Between $\alpha = 6$ and 18 deg. the data pairs are oriented almost vertically indicating no increase of lift in spite of flap area addition; therefore the L/D improvement is purely from drag reduction in this range. As the angle of attack exceeds 18 deg. the data pairs begin to lean towards the horizontal, implying that now the L/D increment is more due to lift increase from the extra flap area. This distinct change in the aerodynamic mechanism signals the lifting-off of the vortex from the flap to the wing (see fig. 2, E).

The pitching-moment characteristics of the wing are not significantly changed by the vortex flap (fig. 4). This is another favorable aspect of the inverse-taper flap which limits the movement of the area center relative to the center of gravity.

A parameter indicative of the drag-reduction effectiveness of the vortex flap is $\xi = C_T \cos \alpha / C_N \sin \alpha$, which relates the forward component of leading-edge thrust to the drag component arising from the normal force. Through ξ the lift-dependent drag characteristics are properly emphasized over the unrealistic drag contribution of model construction peculiarities (such as flap attachments) which are unrepresentative of full-scale and tended to be rather crude on the exploratory models used in the present tests. The parameter also provides convenient theoretical bounds viz. full leading-edge thrust in potential flow giving $\xi = 0.6$ for the basic delta and $\xi = 0$ with zero thrust in fully-separated flow, against which the vortex flap performance may be assessed. Balance measurements converted to ξ (shown in fig. 5) clearly bring out the effectiveness of vortex flaps as a function of angle of attack, and also confirm that the inverse-taper configuration performs competitively with the constant-chord flap of nearly 50-percent larger area.

The use of trailing-edge flaps for lift increment on tail-less delta aircraft, constrained by trim-drag considerations in the past, is now feasible in view of relaxed static stability and active-

control developments. The reduction in angle of attack at a given lift coefficient permitted by trailing-edge flaps leads to net drag reduction on the basic delta wing, as shown in fig. 6. With vortex flaps on, a quite significant additional benefit results at the higher lift coefficients. The leading-edge upwash associated with increased circulation due to trailing-edge flaps enhances the vortex flap thrust potential at low angles of attack, the result being a uniquely efficient low-speed configuration for slender wings. There is also some indication in the limited experimental data that trailing-edge flaps may be somewhat more effective in combination with vortex flaps which promote chordwise attached flow on the wing as opposed to the strong spanwise flow induced by the basic delta vortices (see fig. 1).

An adaptation of the vortex flap concept in which the flap is deployed on the upper surface of the wing, as shown in fig. 7, was briefly investigated on the 74-deg. delta wing. The object was to evaluate the upper-surface vortex flap as a means to augment roll control at high angles of attack when conventional elevons and spoilers are degraded by leading-edge flow separation on slender wings.

A distinctive feature of the upper flap is an inboard vortex fed by the shear layer leaving the free edge of the flap, in addition to the flap vortex as before whose position (adverse or favorable) is governed by angle of attack, fig. 7. In the relevant 'high' angle of attack case, a redistribution of lift caused by the flap vortices moves the center of lift on the wing panel farther outboard. Accordingly when the upper flap is raised only on one side, the resulting asymmetry of span loading generates a rolling moment. Preliminary results presented in fig. 8 show that:

i) Rolling moment coefficient increases with C_L implying that roll power is maintained at low speeds,

ii) Associated yawing moment remains favorable, and

iii) Drag penalty is negligible because of vortex thrust on the flap.

When used in combination with conventional elevons, the upper vortex flap appears to produce a synergistic effect on roll power at lift coefficients above 0.6, fig. 9. Such an effect could arise from induced suction of the inboard vortex flowing over the down-deflected elevon.

The upper vortex flaps may be deployed in a symmetric mode producing longitudinal characteristics typified by the results shown in fig. 10. The large drag force generated at low lift coefficients (due to adverse separation, fig. 7, A) may be utilized for rapid and controlled deceleration from high speeds, with no trim change as evident from the pitching-moment data. The steady flow field associated with the vortex flap should result in exceptionally low levels of buffet and wake-excitation of empennage structures when compared with conventional airbrakes.

60-Deg. Planar Delta Wing

Since the flap vortex depends on the leading-edge sweep for stability and persistence, the question arises whether the vortex flap concept is workable on wings with smaller sweep angles. A systematic investigation of the sweep effect has not been so far conducted. However, results of limited tests on a 60-deg. cropped delta wing model (details of which are given in ref. 2) show that the vortex flap is still effective, fig. 11. Reduced sweep angle combined with a generous leading-edge radius on this basic wing raised the angle of attack for separation and also retained a larger residual leading-edge suction after separation, in comparison with the 74-deg. delta. Consequently, the L/D improvement provided by the vortex flap in this case is relatively less marked. A better appreciation of the vortex flap effectiveness is perhaps obtained in comparison with the calculated zero-suction L/D curve plotted in fig. 11, which would be more representative of a wing with realistic leading-edge radius.

The vortex flap performance at C_L greater than 0.4 again appears to be rather insensitive to flap deflection angle in the range 15 deg. to 45 deg. The pitching-moment characteristics however are distinctly better at 15 deg. and 30 deg. deflection, whereas with 45-deg. flap the pitch-up behavior of the basic wing still is evident. These data illustrate how the vortex flap setting may be selected from longitudinal stability considerations without significantly compromising L/D performance.

The pressure-instrumented 60-deg. delta model provided an opportunity to monitor the upper-surface flow conditions in the vicinity of the leading-edge, with and without the 30-deg. vortex flap. Upper-surface chordwise pressure distributions at 57 percent semi-span station are presented in the left-half of fig. 12 for 13 deg. and 16 deg. angles of attack. These distributions correspond to consecutive test points just before and just after separation onset respectively at the selected semi-span position on the basic wing. The sudden collapse of the high suction peak and loss of subsequent pressure recovery is typical of leading-edge stall. With the vortex flap on, the suction peak at α = 13 deg. is markedly reduced and an attached-flow condition indicated at the leading-edge (as confirmed by tuft and oil-flow visulizations), with little change occurring at the next angle of attack. These observations are in accord with the vortex flap flow pattern postulated in fig. 2, D.

The variation with angle of attack of upper-surface pressure at a rear inboard position is shown in the right-half of fig. 12. The basic-wing data show a typical rapid increase in suction following leading-edge separation and vortex onset at about 10-deg. angle of attack. With the vortex flap on, the appearance of vortex-induced suction is delayed almost to α = 20 deg.

Further evidence of the ability of vortex flap to hold 'down' the vortex to higher angles of attack is contained in the lateral-directional balance data at zero side slip, shown in fig. 13. The incremental rolling and yawing moment coefficients (relative to the nominal values at zero angle of attack) indicate sudden departures/oscillations in the α-band corresponding to the spread of leading-edge separation across the semi-span, which generally does not occur symmetrically, on the two

wing panels. These gyrations are effectively suppressed by the vortex flap. A relatively mild rolling-moment onset at about 20-deg. angle of attack is consistent with the pressure-coefficient departure already noted in fig. 12 and signals the migration of the vortex over to the wing.

Supersonic Cruise Configuration

The first evaluation of the vortex flap on a realistic aircraft configuration was carried out during 1979 on a 3-percent scale model of a NASA Langley supersonic-cruise concept. This model has been employed recently in a comprehensive test program emphasizing the low-speed aerodynamic problems and possible solutions including leading-edge deflection effects (ref. 3) and thus was an appropriate vehicle for a competitive assessment of the vortex flap.

A break in the leading-edge sweep angle on this arrow-wing configuration afforded the opportunity to investigate a two-segment flap arrangement one on either side of the discontinuity; the study was extended to include a four-segment vortex flap also. Salient results of this investigation, reported in ref. 4, are worth recalling here in view of the uniqueness of the segmented flap concept.

Smoke visualization was conducted initially to observe vortex formation on the four-segmented flap. A typical photograph of the cross-flow plane illuminated by a thin sheet of light shows the vortex core on the second flap segment, fig. 14. Similar vortices were observed on the other segment also.

The performance of segmented vortex flaps is compared with that obtained using an 'optimum' leading edge. This was an experimentally determined geometry for attached flow at 10-deg. angle of attack, with leading-edge deflection increasing continuously from 16-deg. inboard to 50-deg. outboard (ref. 3). Considering that this optimum leading edge was more an aerodynamic ideal than a realizable design, a comparable L/D performance produced by the much simpler (and unoptimized) two-segment vortex flap at $C_L > 0.3$ is remarkable. The four-segment version with 40 percent less flap area is only marginally less effective. These initial results suggest that with the increased optimization opportunities available with multi-segment vortex flaps (such as planform shaping, spanwise tailoring of segment area and deflection area and deflection angle etc.), potential for further performance improvement will exist.

The high level of effective dihedral characteristic of highly-swept wings requires corresponding high degree of lateral control in order to meet the cross-wind landing requirement. Roll control however is limited on slender wing aircraft at low speeds and therefore a reduction in lateral stability at the landing lift coefficients is desirable. With segmented vortex flaps, a significant reduction in the roll derivative $dC_l/d\beta$ has been measured on the present configuration, fig. 16. which emerges as another attractive feature of the vortex flap concept.

IV. Concluding Remarks

A selection of experimental results has been presented highlighting the potential of vortex flaps in improving the low-speed aerodynamics of highly-swept delta wings and of a typical slender supersonic cruise configuration. The research so far primarily has been exploratory with emphasis on exposing various basic facets of the concept, at the same time keeping in sight the need for practical simplicity. While the main objective was drag reduction at high lift coefficients, other important low-speed problems such as stability and control have also been addressed. The results show that the vortex flap as an effective flow manipulator can powerfully influence the efficiency and controllability of slender wings when operating in an aerodynamic environment governed by leading-edge separation and vortex flow. Further research is continuing to fully understand and develop the potential of the device and to generate an analytical basis for design optimization in practical applications.

References

1. Rao, D. M.: Leading Edge Vortex Flap Experiments on a 74-Deg. Delta Wing. NASA Contractor Report 159161 (1979).

2. Rao, D. M., and Johnson, Thomas D., Jr.: Subsonic Wind Tunnel Investigation of Leading-Edge Devices on Delta Wings (Data Report). NASA Contractor Report 15920 (1979).

3. Coe, Paul L., and Huffman, Jarrett K.: Influence of Optimized Leading-Edge Deflection and Geometric Anhedral on the Low-Speed Aerodynamic Characteristic of a Low-Aspect-Ratio Highly Swept Arrow-Wing Configuration. NASA TM 80083 (1979).

4. Rao, D. M.: Exploratory Subsonic Investigation of Vortex Flap Concept on Arrow Wing Configuration. NASA CP 2108 (Part I), pp. 117-129 (1979)

Symbols (NOTES)

A	Wing Reference Area
A_f	Vortex Flap Area
AR	Aspect Ratio
C_D	Drag Coefficient
ΔC_D	$C_D - C_l^2/\pi$ AR
C_L	Lift Coefficient
C_l	Rolling Moment Coefficient (body axis)
ΔC_l	$C_l - C_{l(\alpha=0)}$
C_{l_β}	$dC_l/d\beta$
C_m	Pitching Moment Coefficient
C_N	Normal Force Coefficient
C_n	Yawing Moment Coefficient
ΔC_n	$C_n - C_{n(\alpha=0)}$
C_P	Pressure Coefficient
C_T	Thrust Coefficient signifying forward Chordwise Force
C_Y	Side Force Coefficient
L/D	Lift/Drag Ratio
α	Angle of Attack (deg.)
β	Angle of Yaw or Sideslip (deg.)
δ_T	Trailing Edge Flap Deflection (deg.)
ξ	$C_T \cos \alpha / C_N \sin \alpha$

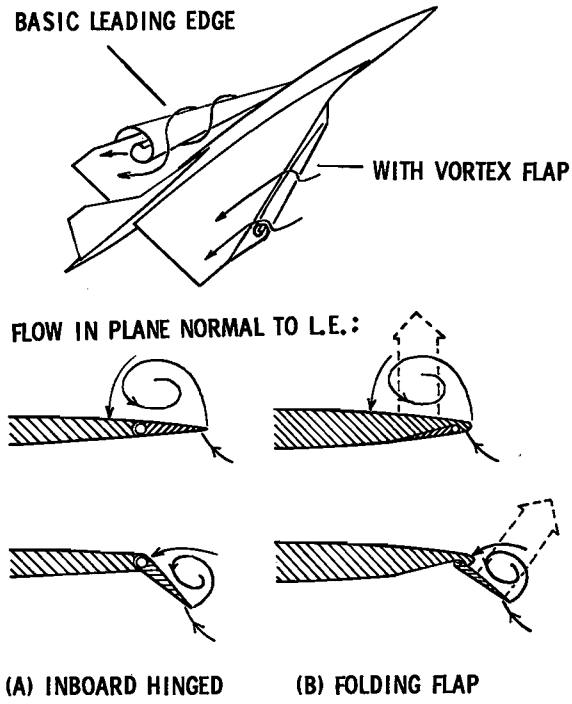

Fig. 1 The Vortex Flap Concept.

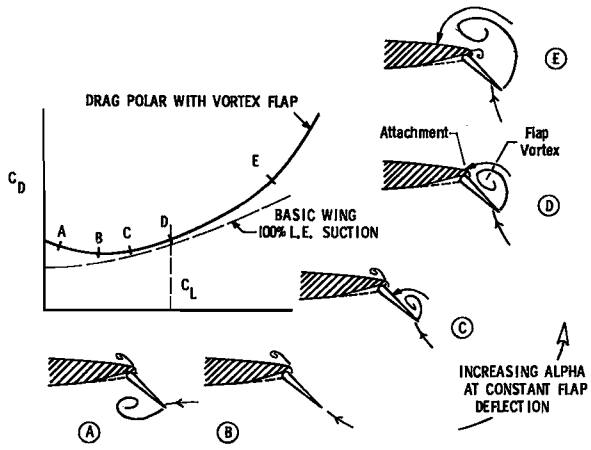

Fig. 2 Flow Patterns on vortex Flap.

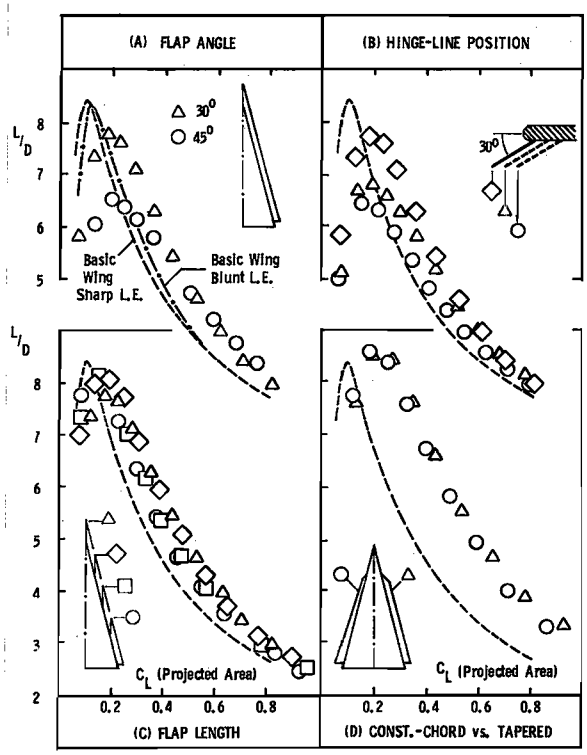

Fig. 3 Effect of Vortex Flap Variations on 74-Deg. Delta Wing Performance.

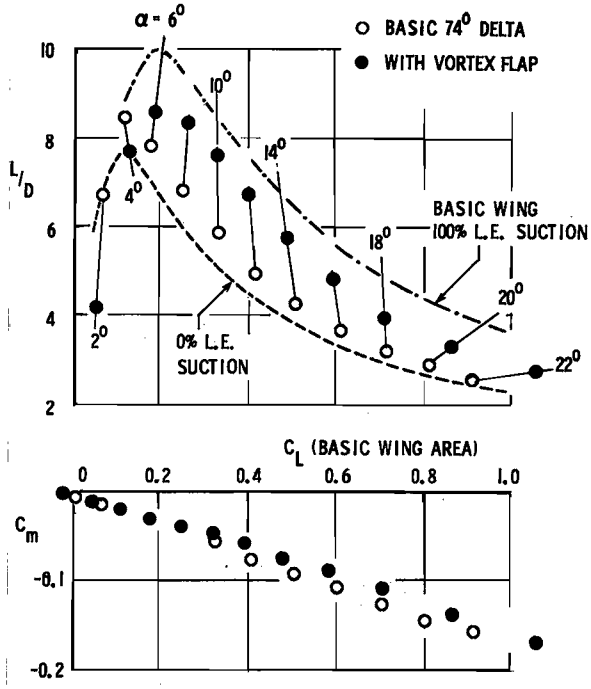

Fig. 4 Longitudinal Characteristics of 74-Deg. Delta with and without Vortex Flap.

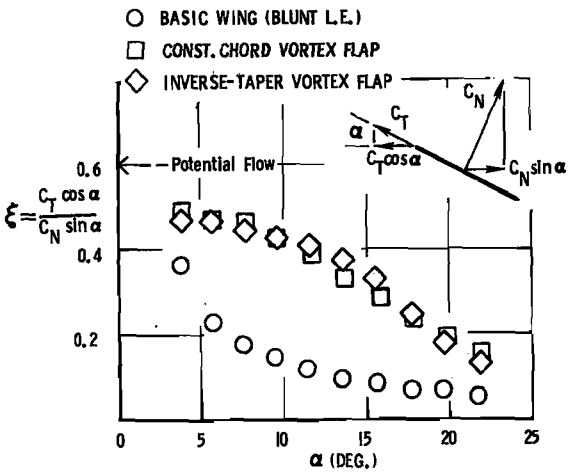

Fig. 5 Thrust Effectivenesss of Vortex Flaps on 74-Deg. Delta Wing.

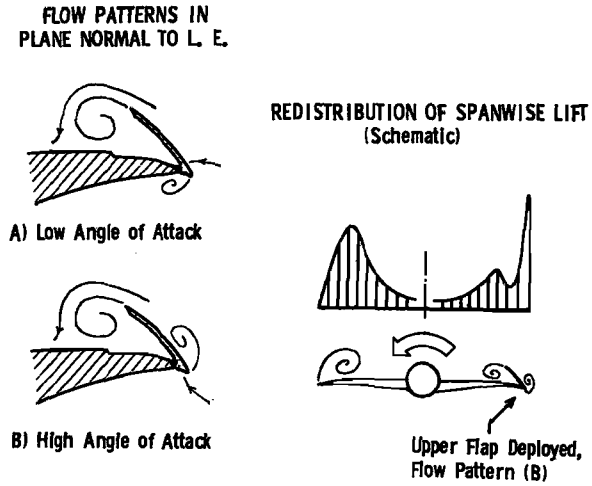

Fig. 7 Upper Surface Vortex Flap for Roll Control.

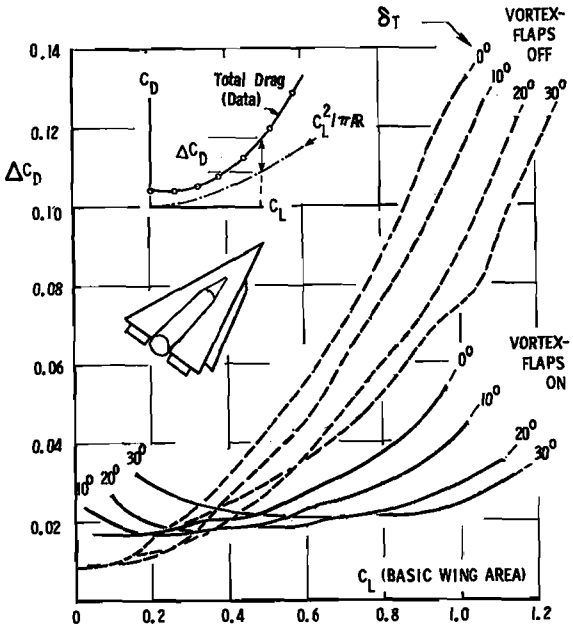

Fig. 6 Trailing Edge Flap Effect on Drag of 74-Deg. Delta Wing with and without Vortex Flap.

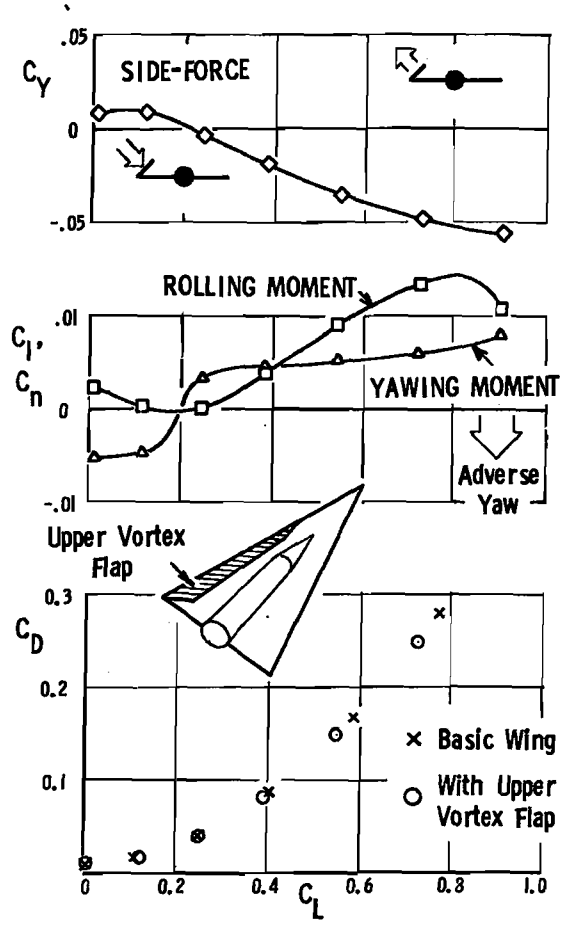

Fig. 8 Typical Aerodynamic Characteristics of 74-Deg. Delta Wing with Upper Vortex Flap.

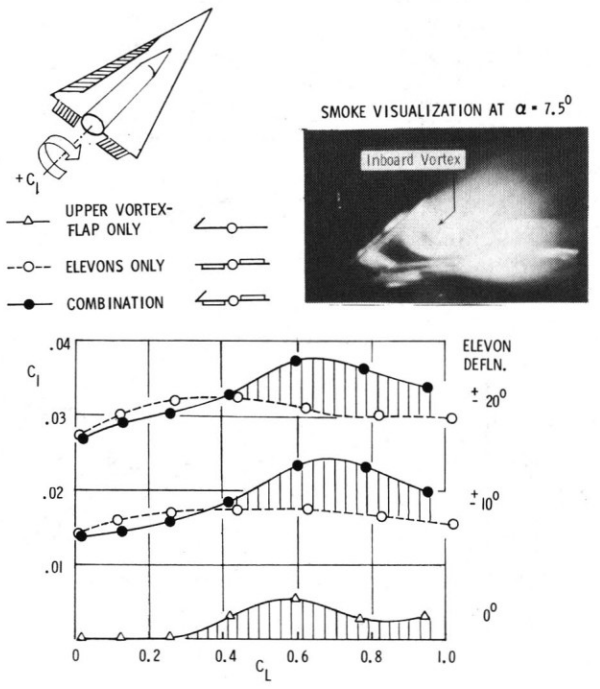

Fig. 9 Augmentation of Elevon Roll Power with Upper Surface Vortex Flap.

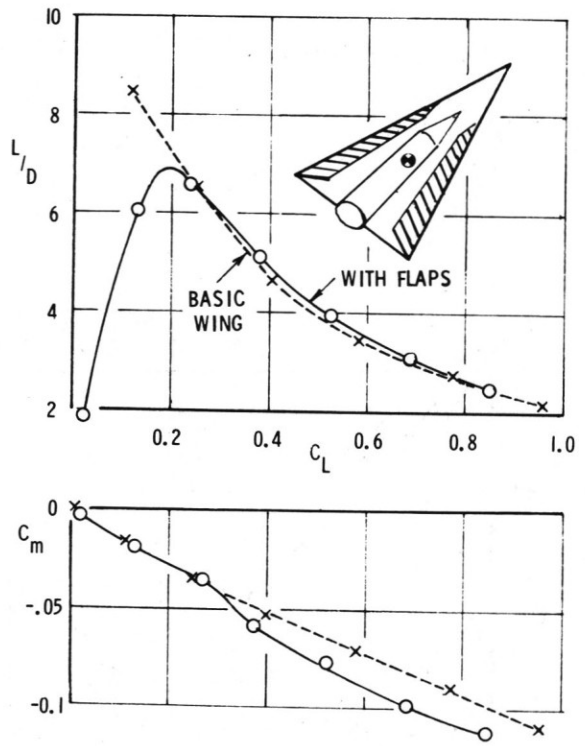

Fig. 10 Longitudinal Characteristics of 74-Deg. Delta with Symmetric Upper Surface Vortex Flaps.

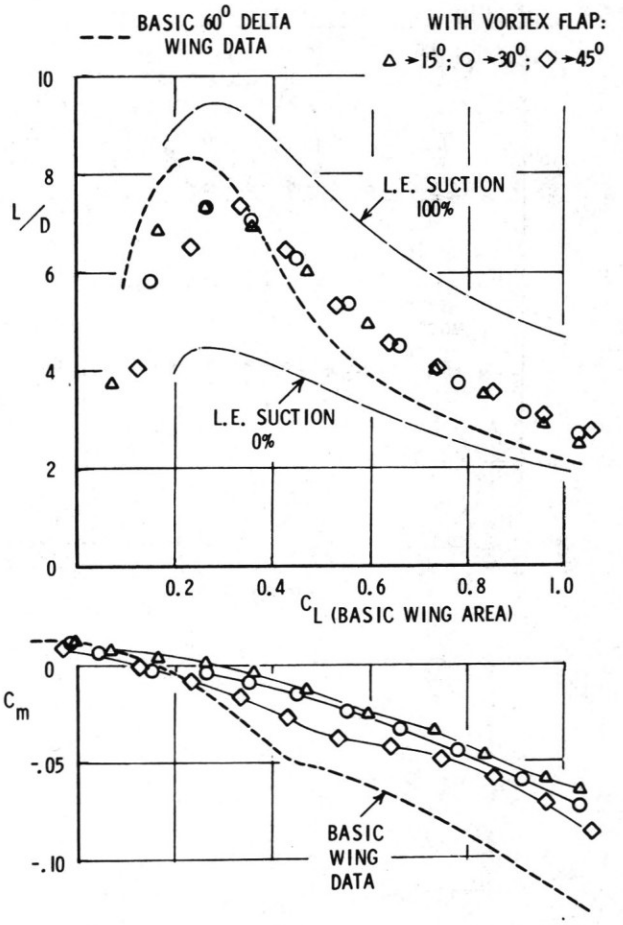

Fig. 11 Performance and Longitudinal Stability Effects of Vortex Flap on 60-Deg. Delta.

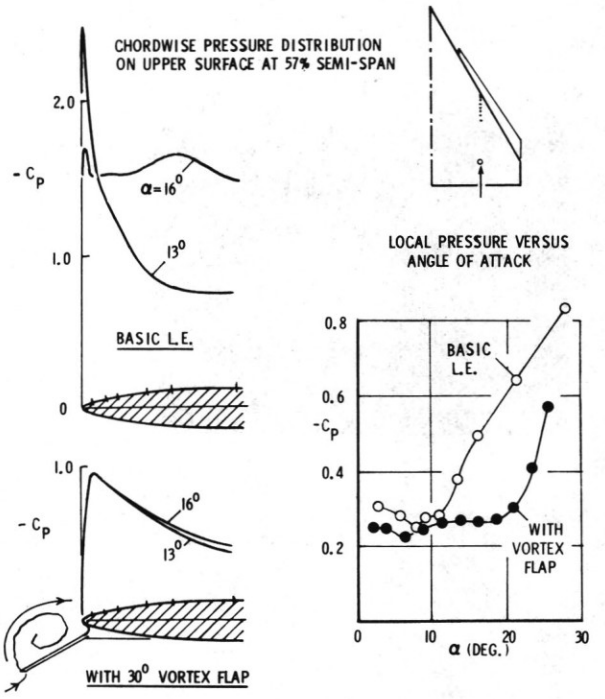

Fig. 12 Upper-Surface Pressure Distribution on 60-Deg. Delta showing Vortex Flap Influence.

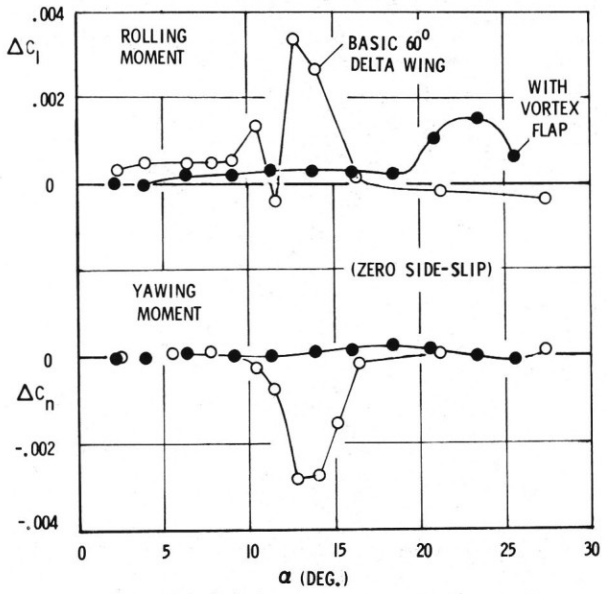

Fig. 13 Vortex Flap Effect on Rolling and Yawing Moment at Zero Sideslip on 60-Deg. Delta.

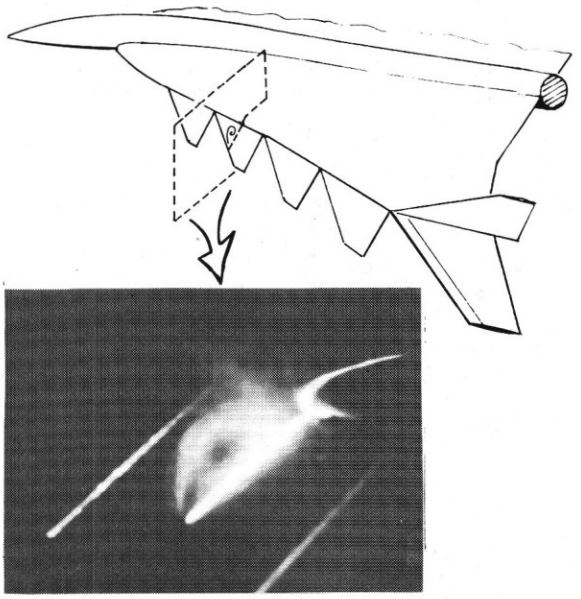

Fig. 14 Smoke Visualization of Vortex on Segmented Flap.

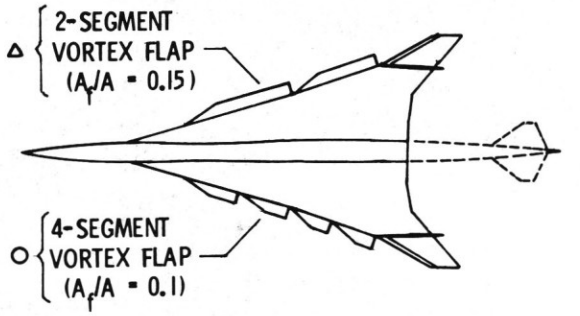

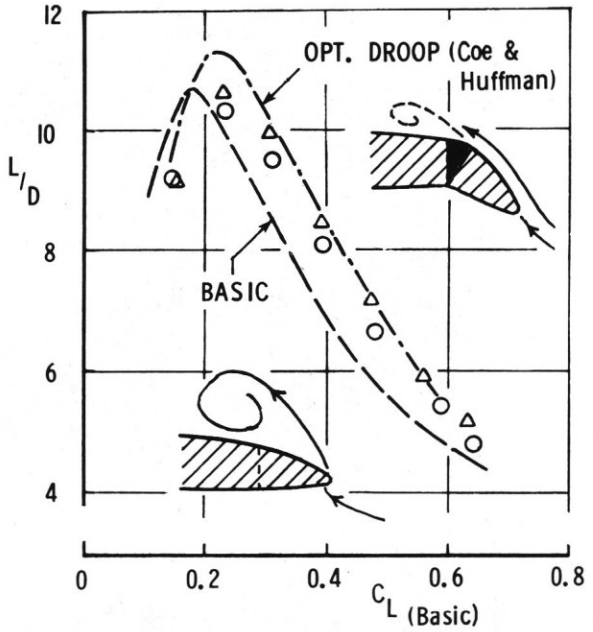

Fig. 15 Segmented Vortex Flap Performance on Supersonic Cruise Configuration.

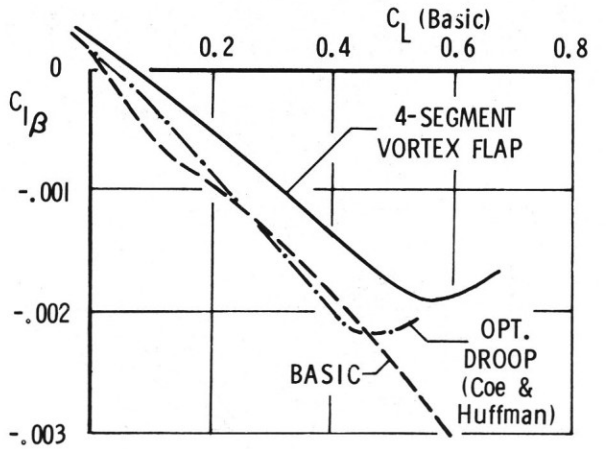

Fig. 16 Lateral Stability of Supersonic Cruise Configuration with Segmented Vortex Flap.